CHAPTER 3

NUMERICAL EXAMPLES

This chapter presents results of several test problems that are used to verify the methodology. The problems are either taken from literature for direct comparison or created specifically to demonstrate the advantages of the Displacement Based Optimization (DBO).

For all the problems solved by DBO in this chapter, Sequential Quadratic Programming (SQP) or BFGS solver of the commercial code DOT (VR&D, 1999) is used for outer level problem depending on whether there are stresses constraints or not. In general, most problems hereafter do not have outer level constraints except displacement bounds. In the presence of limited ductility of the material, bounds on the plastic multipliers (Kaneko and Maier 1981) could be imposed. These bounds on the plastic multipliers are equivalent to stress constraints. It is not the intention here to focus on stress constraints, which otherwise are helpful for DBO since they will provide feasible region information for the outer level searching. Thus, the outer level optimization problem in the

DBO setting becomes unconstrained minimization for most of the problems discussed hereafter. The BFGS unconstrained solver of DOT is used for solving such problems. For the inner level problem, Dense Revised Simplex Linear Programming code of IMSL (Visual Numerics, Inc., 1997) is used.

Robustness and efficiency are emphasized in the discussion of all test problems. Especially, computing time is given for all DBO examples. Some are compared to computing time available from the other published paper. In DBO, analytical gradients that are described earlier in section 2.5 are used instead of computing finite difference gradients. The program developed for DBO links with IMSL math library code to use its Linear Programming solver. The program also includes a general-purpose linear elastic finite element source code to obtain the stiffness matrix information for computing analytical gradient and initial displacement response. These initial displacements are used as starting values for the outer level optimization variables. It is also valuable to point out that such a code may not demonstrate precisely time saving gain by investigating small size academic examples.

3.1 THREE-BAR TRUSS

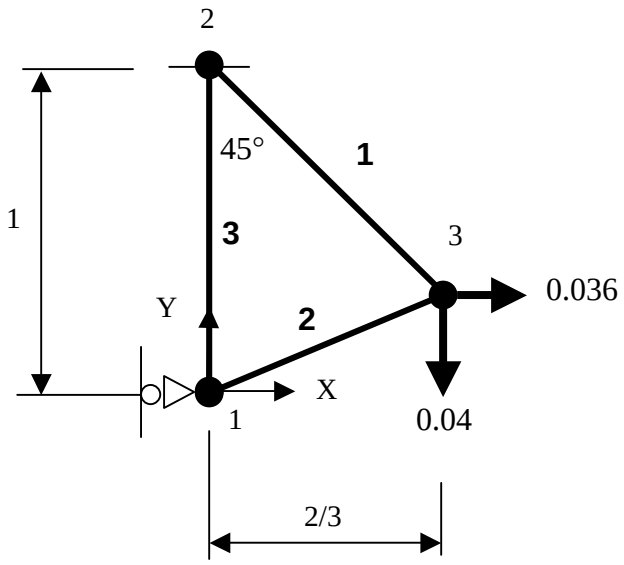

Fig. 3.1: 3-Bar Truss (Cinquini and Contro 1984)

The 3-bar truss design example Shown in Fig. 3.1 was used by Cinquini and Contro (1984) and recently by Tin-Loi (1999). For all truss elements in the structure linear strain hardening material law applies. Under the formulation of the holonomic, elastoplastic analysis problem proposed by Kaneko and Maier (1981), the design problem behind truss-like structures becomes a class of Nonlinear Programming problem with complementarity constraints. The paper of Cinquini and Contro developed an optimal criteria approach to obtain an optimum solution to this 3-Bar truss. The paper of Tin-Loi employed a smoothing scheme for complementarity constraints and got the same solution for this 3-bar.

For all papers discussed above, minimum volume is sought by optimizing three design variables, i.e., three cross-sectional areas a_i of the bars. The following parameters are assumed:

Normalized Young's modulus E = 1, yield limit (tension and compression) σ_y = 0.0015E, the hardening modulus $H = E/6$, vertical displacement of node 3 is prescribed as exactly 0.0025 down.

Since there are no stress constraints in the problem, the outer level problem for the DBO is actually an unconstrained minimization. The unconstrained optimizer used is BFGS of DOT optimization software. To satisfy that vertical displacement requirement, DBO simply sets prescribed value to this vertical displacement, thus gets rid of this displacement variable and leaves the design problem in only two displacement design variables space. The initial displacement field is assumed to be the response of a linear elastic finite element analysis from initial member areas. Table 3.1 presents results of DBO as well as previous papers to provide comparison. Iterative history of weight is plotted in Figure 3.2.

Table 3.1 Optimum Results For 3-Bar Truss

Element index	Initial Areas	DBO CSAs	Stress/σ_y	Cinquini & Contro CSAs	Stress/σ_y	Tin-Loi CSAs
1	20	35.221	1.0356	35.4	1.03	35.620
2	20	2.9947	–0.6645	3.0	–0.66	2.796
3	20	1.3406	0.6542	1.3	0.66	1.251
Optimum Weight		36.779		36.9		36.918
# of Iterations		5		–		6
Time (sec)		0.60		–		0.97

For DBO, obtained optimum displacements are –0.99614E-3, –0.78881E-4, and –0.0025 for the degrees of freedom of node 1 Y direction, and node 3 X and Y directions, respectively.

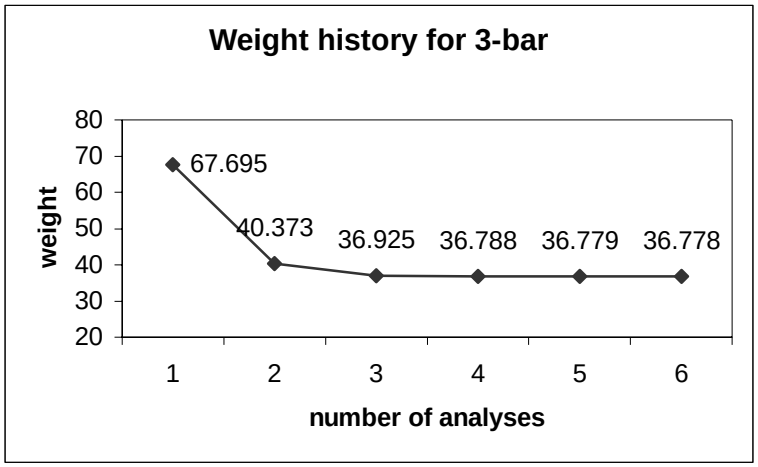

Fig. 3.2 Weight Iterative History Of 3-Bar Truss

In order to test robustness, the DBO approach is also used to solve another case of the problem, i.e., taking all three free degree of freedom as displacement design variables. The absolute values of upper and lower bounds of three displacements are set to 0.01. Without any difficulty, the DBO obtained an optimum weight of 21.453 from initial weight of 65.135 after 5 iterations. The optimum areas are (20.479, 2.0039, 0.65223) with corresponding optimum displacement (–0.47859E–2, 0.13657E–2, –0.10000E–1). At the optimum, the third displacement variable reached its lower bound of –0.01.

Results of Tin-Loi by the SAND approach (see Chapter 1) gave impressively short computational time for this example using a code developed in GAMS

(Tin-Loi, 1999) modeling language that is very efficient. This GAMS code was run on a Win95 based PC of 333 MHz Pentium II. DBO FORTRAN code results are generated on a Windows 98 PC with a 400 MHz Pentium II processor. When problem size increases, it is envisioned that DBO should demonstrate considerable gain in computational time. Furthermore, time saving could be particularly large if comparable results are generated by solving a standard structural optimization problem that includes the expense of one costly nonlinear finite element analysis for each cycle of optimization iteration.

3.2 SIX-BAR TRUSS

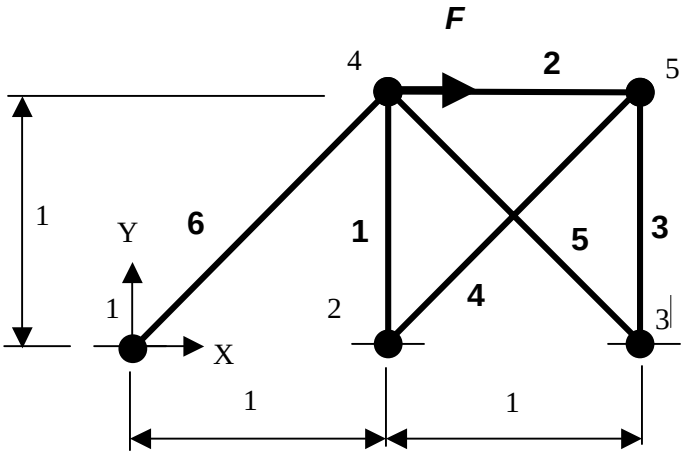

Fig. 3.3: 6-Bar Truss (Kaneko and Maier 1981)

The 6-bar truss, used by Kaneko and Maier (1981) and Tin-Loi (1999), is shown in Fig. 3.3. Each bar of the structure is assumed to have a single elastic-perfectly-plastic yield mode in compression and an infinitely linear elastic material law in tension. The transition point from elastic to perfectly-plastic mode is the yield limit point. The design variables for optimization were formulated in terms of the compressive plastic resistances of the members. The resistances are physically connected to Euler buckling load of the bars. Kaneko and Maier (1981) explained that the Euler buckling load representing yield mode of the *i*th bar is $\pi^2(EI)_i L_i^{-2}$ in the plane of the axes. 'Sandwich' cross sections with given depth h_i are assumed for all bars, so that $I_i=0.5h_i^2A_{i,}$ where A_i being the area of each of the flanges which form stress-carrying parts of the symmetric sandwich section in the bar i. It follows that resistances and weight will be proportional to member areas A_i. As a

result, the objective function was still expressed as a linear function of 6 areas design variables. The following normalized parameters are assumed (note that Kaneko and Maier didn't present the units for the material data):

Young's modulus E_i=3 for bars i=1, 2, 3 and E_j =2$\sqrt{2}$ for j=4, 5, 6;

Yield limit (tension and compression) $(\sigma_y)_i$ = 3 and $(\sigma_y)_j$ = 2;

Absolute values of all nodal displacements were less than or equal to 4;

Node 4 X direction has a positive load F=9 as shown in Fig. 3.3;

Resistances are defined as r_i=3a_i and r_j=2a_j;

The objective function is expressed as $\boldsymbol{l}^T\boldsymbol{r}$, where vector $\boldsymbol{l}$=(l_1, l_2, l_3, l_4, l_5, l_6) is composed of element length of all bars and vector $\boldsymbol{r}$=(r_1, r_2, r_3, r_4, r_5, r_6) the element resistances.

Table 3.2 presents results by DBO as well as from the above two papers. Iterative history of cost function is plotted in Fig. 3.4. The results obtained by DBO and Tin-Loi gave the same good optimal two bars (5 and 6) supporting the loading. All the remaining bars have zero values of areas. Kaneko and Maier clearly got a relatively heavier optimum design compared to results by the DBO and by Tin-Loi.

Table 3.2 Optimum Results For 6-Bar Truss

Element index	Initial Areas	DBO Resistances	Stress/σ_y	Kaneko&Maier Resistances	Tin-Loi Resistances
1	1.0	0.0	–	1.410	0.0
2	1.0	0.0	–	1.410	0.0
3	1.0	0.0	–	1.410	0.0
4	1.0	0.0	–	5.326	0.0
5	1.0	6.364	–1.00074	0.470	6.364
6	1.0	1.367	4.656	0.470	1.367
Optimum Weight		10.933		13.091	10.933
# of Iterations		7		–	6
Time (sec)		1.10		–	1.36

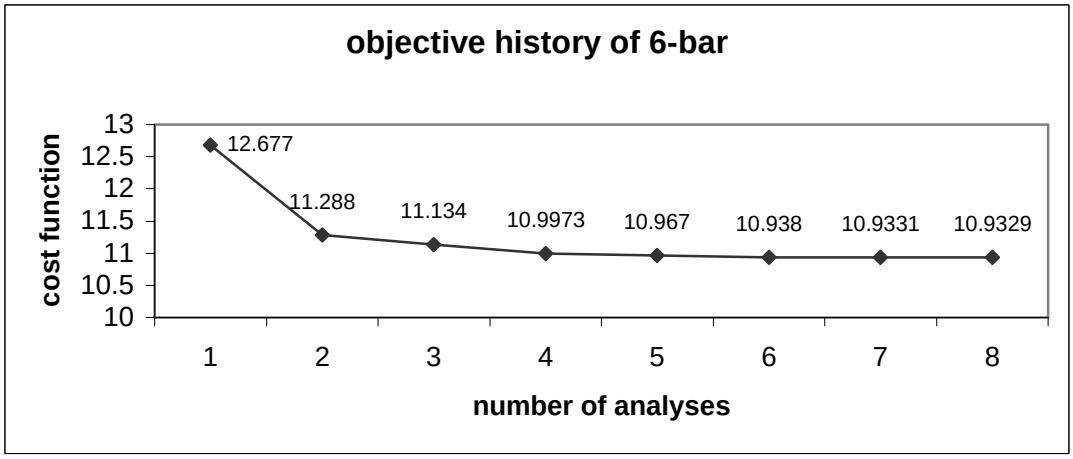

Fig. 3.4 Objective Iterative History Of 6-Bar Truss

For DBO, obtained optimum displacements are 4.0, 2.5847, 2.7693 and –0.69231 for the degrees of freedom of node 4, X and Y directions, and node 5, X and Y directions, respectively. The displacement variable of node 4 X direction reached its upper bound 4.0. This upper bound constraint is the only active constraint for minimum weight. It should also be noted that the values of two displacements of

node 5 are not zero at the optimum. From a physical point of view, some doubt may be cast on the results since optimal solution has deflection of node 5 that is attached with truss elements of zero areas. However, in the DBO approach such a result is still acceptable because the inner problem inversely designs the structure from known displacement to determine the unknown areas. To analyze results, any displacement of no mechanical interest is simply neglected.

Another noticeable aspect is the occurrence of zero areas of members that may create problems for finite element model of the structure. To prevent numerical difficulties, both the two classical papers restricted the design variables to be greater than a small number, say 10E-6. By this way, no member is completely removed from the discretized model. For large size problems applying zero lower bounds to design variables, the classical approach will face possible ill-conditioning of the stiffness matrix. On the contrary, DBO inherently do not need such preventive mechanism for zero lower bounds case. The members can be totally removed from the structure. This is one advantage of DBO which can easily locate a topologically best structure responding very well to external loading. This academic example gives an evidence for such a perspective.

To gain further insight to the same problem, purely linear elastic case is solved to investigate and compare results. Everything remains the same except applying infinite linear elastic behavior for compression of bars. DBO obtained an optimum objective 6.364 from initial 7.354 after 4 iterations, using the same starting areas as that of the nonlinear case. The optimum areas are (0.0, 0.0, 0.0, 0.0, 1.125, 1.125) and optimum displacement are (4.0, -0.37921E-5, 2.7693, -0.69231). Stresses of bars 5 and 6 at optimum are $-2.828\sigma_y$ and $2.828\sigma_y$. The

reason why linear optimum objective is lower than nonlinear is that no stresses constraints are applied to either the linear or the nonlinear case. The perfectly-plastic mode in compression surely weakens the structure so that the resultant optimum weight of nonlinear structure is heavier.

3.3 TEN-BAR TRUSS

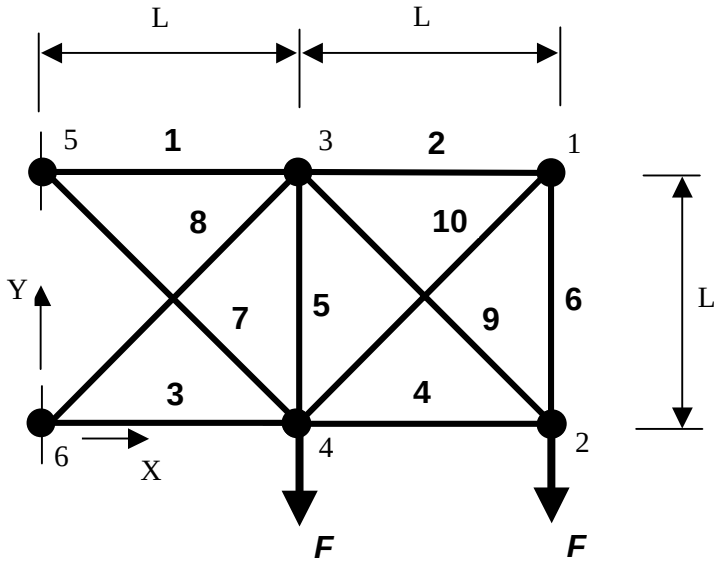

Fig. 3.5: 10-Bar Truss (Schmit and Miura 1976)

The popular ten-bar truss structure, shown in Fig. 3.5, is used to experiment with the DBO methodology as it applies to nonlinear problems. This section is divided into three parts. The first part presents results for a pure linear structure. The second part deals with elastic-perfectly-plastic case and compares results with those of Limit Design approach (Haftka & Gurdal, 1992). The follow-up third part gives new results for Linear Strain Hardening and general curve nonlinear material cases. The purpose of presenting linear results lies in the fact that, it not only provides nonlinear results their linear counterpart to be compared with but also set a metric to show how much computer time is expanded when DBO is extended to solve nonlinear structure compared to the linear one.

3.3.1 TEN-BAR TRUSS: LINEAR ELASTIC CASES

The minimum weight problem of linear elastic ten-bar with stresses constraints was solved by both Schmit and Miura (1976) and Vanderplaats and Salajegheh (1989) using approximation concepts. Their results, the best available in literature, required the level of ten structural analyses to obtain optima. DBO solved this problem efficiently and accurately using Sequential Linear Programming for outer level optimizer (S. Missoum et al, 1998). Here numerical experiments were performed for more cases using Sequential Quadratic Programming. The results will provide necessary data to study and compare results of nonlinear cases of this ten-bar.

Some assumed parameters are given by:
Young's modulus E=10^7 *psi*, density ρ=0.1 *lbs/in*^{3}, Length L=360″
Three different kinds of cases are considered:
Case A: allowable stresses for all bars is ±25000 *lbs/in*^{2},
minimum areas for all bars are 0.1 *in*^{2}
Case B: same as case A except allowable stress for bar 9 is ±50000 *lbs/in*^{2}
Case C: same as case A except minimum areas for all bars are 0.0 *in*^{2}
The structure has one loading condition of F=100000 *lb* as shown in Fig. 3.5.

Table 3.3 presents results of three cases by DBO and comparable results from classical literature. It is clear that number of analyses by DBO is on the same magnitude as those by Approximation Concepts (AC) approach. AC usually creates high quality sequential local approximate problems to improve efficiency of searching. DBO does not create any approximate problems but searches

directly in displacement design space. The optimization process of DBO was carried out without applying any move limit strategies. This shows that DBO is quite insensitive to move limits.

Table 3.3 Results for linear elastic 10-Bar truss

CSAs	Initial Areas	Case A DBO	Case A SM[1]	Case A Fully Stressed Design	Case B DBO	Case B MG[2]	Case B SM	Case B VS[3]	Case C DBO	Case C Fully Stressed Design
1	20.0	7.9309^{+}	7.938	7.93787	7.90 $^{+}$	7.90	7.90	7.90	8.0 $^{+}$	8.0
2	20.0	0.1006	0.1	0.10	0.10 $^{+}$	0.10	0.10	0.10	0.0	0.0
3	20.0	8.0690^{-}	8.062	8.06213	8.10 $^{-}$	8.0999	8.10	8.10	8.0 $^{-}$	8.0
4	20.0	3.9309^{-}	3.938	3.93787	3.90 $^{-}$	3.8999	3.90	3.90	4.0 $^{-}$	4.0
5	20.0	0.10	0.1	0.10	0.10	0.10	0.10	0.10	0.0	0.0
6	20.0	0.10	0.1	0.10	0.10 $^{+}$	0.10	0.10	0.10	0.0 $^{+}$	0.0
7	20.0	5.7544^{+}	5.745	5.74472	5.7983^{+}	5.7983	5.80	5.80	5.6569^{+}	5.6569
8	20.0	5.5592^{-}	5.569	5.56899	5.5154^{-}	5.5154	5.52	5.51	5.6569^{-}	5.6569
9	20.0	5.5592^{+}	5.569	5.56899	3.6769	3.6769	3.68	3.67	5.6569^{+}	5.6569
10	20.0	0.1201	0.10	0.10	0.1414^{-}	0.1414	0.14	0.14	0.0 $^{-}$	0.0
Weight lb	8392.9	1593.5	1593.23	1593.18	1497.6	1497.6	1497.6	1497.4	1584.0	1584.0
Iter. No.		10	16	–	8	345	16	7	2	–
Time(sec)		1.37	–	–	0.93	–	–	–	0.28	–

$^{+}$ the element stress on that bar meets its tension limit.
$^{-}$ the element stress on that bar meets its compression limit.
1: SM is Schmit and Miura.
2: MG is Missoum and Gurdal.
3: VS is Vanderplaats and Salajegheh.

DBO's results of Case C (zero area bounds) required only 2 iterations to obtain optimum. In fact, first iteration has already located the optimum. The second iteration satisfied convergence and stopped the search for the Sequential Quadratic Programming iterations. There are critical stresses at zero areas of member 6 and 10 in Case C. This is because DBO gives optimum displacement field corresponding to optimum design. Stresses are directly computed from the displacement values without the need for any area values.

3.3.2 TEN-BAR TRUSS: ELASTIC-PERFECTLY-PLASTIC CASES

This problem is designed to compare DBO results with popular Limit Design approach. All three cases of 10-bar in section 3.3.1 are used while applying elastic-perfectly-plastic (EPP) behavior for both tension and compression of bars. Transition yielding points from linear elastic to EPP are the allowable stresses used in section 3.3.1. For DBO, the problems in this section again become unconstrained minimization for the outer level problems. Using Mathematica software, a Limit Design program for this truss was developed and used to obtain optimal designs. All results are listed in Table 3.4. The objective function histories of DBO results are plotted in Fig. 3.6 as a function of the iteration numbers.

Comparing the results between DBO and Limit Design, it is observed for two cases of nonzero area bounds that the two approaches got the same optimum weight but different distribution of area values. After careful investigation, it is concluded that there are multiple optima around certain location with same minimum weight values. At least, several different minimum points were produced after the Limit Design program carried out several different runs by using slightly different formats of design variables. In such a situation, DBO captures one optimum with same minimum weight as results of Limit Design have.

Limit Design for EPP structure only needs one Linear Programming run to get its optimum. DBO needs a general iterative process so that it requires more computing time. However, the purpose here is to show the fact that DBO can do everything Limit Design does. Furthermore, from a broader perspective, DBO is

apparently superior to Limit Design because it can consider displacement or stress constraints in a straightforward manner. On the contrary, it is well known that Limit Design framework cannot consider displacement constraints that are almost always necessary for practical engineering design problems.

Table 3.4 Results for 10-bar with elastic-perfectly-plastic material

CSDs	Initial Areas	Case A DBO	Case A Limit Design	Case B DBO	Case B Limit Design	Case C DBO	Case C Limit Design
1	20.0	7.9064	8.0	7.8835	8.02929	8.0	8.0
2	20.0	0.10	0.1	0.10	0.1	0.0	0.0
3	20.0	8.0935	8.0	8.1164	7.97071	8.0	8.0
4	20.0	3.9	3.9	3.9	3.92929	4.0	4.0
5	20.0	0.1	0.1	0.1	0.1	0.0	0.0
6	20.0	0.1	0.1	0.1	0.1	0.0	0.0
7	20.0	5.7891	5.65685	5.8215	5.61543	5.6569	5.65685
8	20.0	5.5245	5.65685	5.4922	5.69828	5.6569	5.65685
9	20.0	5.5154	5.51543	2.7577	2.77843	5.6569	5.65685
10	20.0	0.14142	0.141421	0.14142	0.1	0.0	0.0
Weight (lb)		1591.2	1591.2	1450.80	1450.8	1584.0	1584.0
Iter. No.		29	–	31	–	16	–
Time (sec)		4.39	–	4.84	–	2.72	–

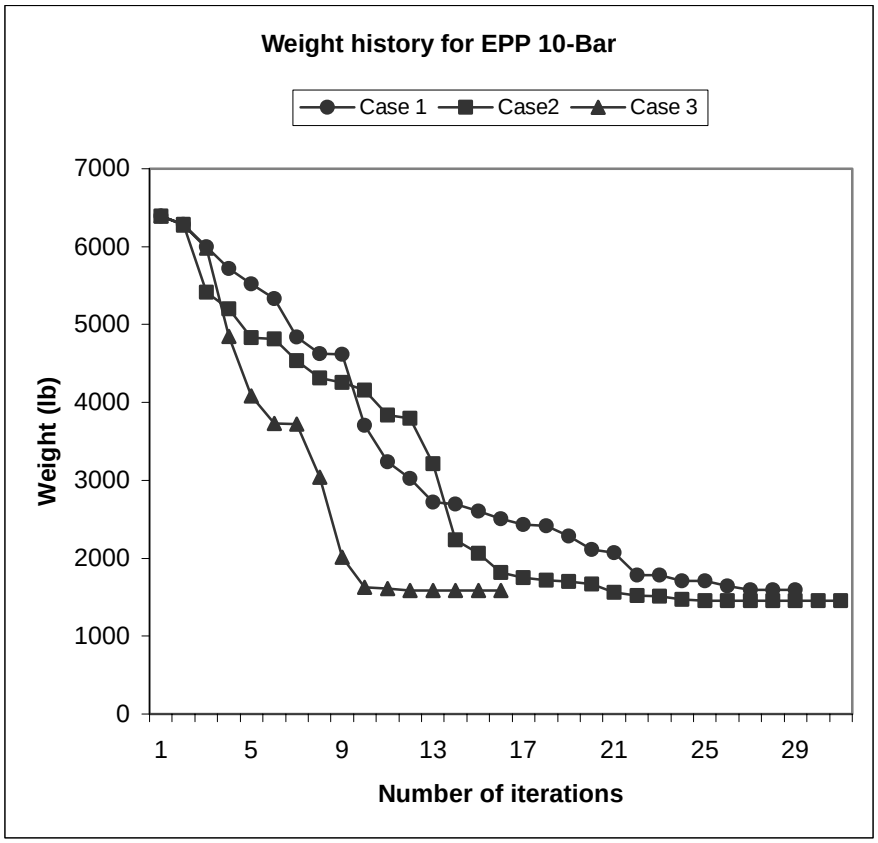

Fig. 3.6 Objective history of 10-bar with elastic-perfectly-plastic material

3.3.3 10-BAR : LINEAR STRAIN HARDENING AND RAMBERG-OSGOOD MODEL CASES

The 10-bar problem with linear strain hardening model and general elastoplastic law are solved here. The choice of empirical equation for general uniaxial stress-strain curve requires special attention. At first, a power law was employed. However, numerical studies showed that power law created computational difficulty when tangential Young's modulus E_t of certain member was computed from a near-zero strain value. In such a case, E_t is near infinite. It is also a fact that power law does not usually fit well at the low-strain and high-strain ends of the stress-strain curve. As a result, another frequently used form due to Ramberg-Osgood (Mendelson 1968), as described in Chapter 2, is used. When *n* is infinite in (2.16) of section 2.3, the Ramberg-Osgood model becomes the EPP model studied in section 3.3.2. In this section, *n* is chosen to be 2. With this assumption, the following equations are used in program:

$$\varepsilon = \frac{\sigma}{E} + K(\frac{\sigma}{E})^2 \;\Rightarrow\; \sigma = \frac{E}{2K}(-1+\sqrt{1+4K\varepsilon}),\quad E_t = \frac{E}{\sqrt{1+4K\varepsilon}} \qquad (3.1)$$

The Ramberg-Osgood model with coefficient K to be 300 is shown with corresponding EPP model in Fig.3.7. Hardening coefficient h (defined in section 2.3) is ½ for Linear Strain Hardening model. All models are applied for both tension and compression of truss members in Case A. Table 3.5 lists optima results while Fig.3.8 shows the objective function history.

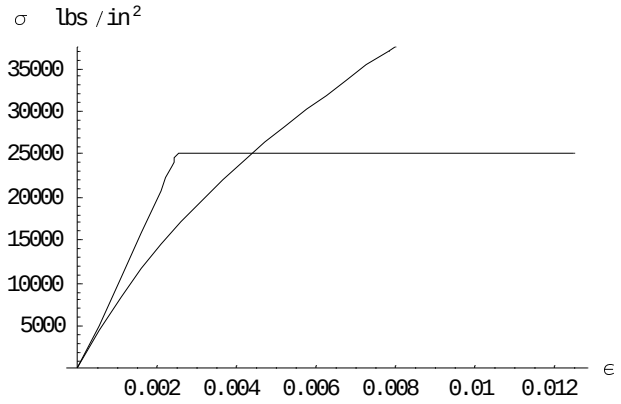

Fig. 3.7 Stress-Strain Curves: Elastic-Perfectly-Plastic v.s. Ramberg-Osgood

Table 3.5 10-bar with Linear Strain Hardening and Ramberg-Osgood Material

Index	Initial Areas	Case A: Areas	Bi-linear Stress/σ_y	Case A: Areas	R-O Stress/σ_y
1	20.0	6.7610	1.2045	9.6306	0.84151
2	20.0	0.10	0.29647	0.1	0.27351
3	20.0	5.9563	–1.3189	8.3988	-0.9401
4	20.0	3.4865	–1.1387	4.7864	-0.82998
5	20.0	0.1	1.7378	0.1	1.316
6	20.0	0.10021	0.29583	0.10435	0.26209
7	20.0	3.0888	1.7653	4.2417	1.2988
8	20.0	4.8691	–1.2036	6.9003	-0.84116
9	20.0	4.9221	1.1407	6.8068	0.82537
10	20.0	0.10855	–0.38622	0.1252	-0.30895
Weight (lb)		1255.4		1752.5	
Iter. No.		32		30	
Time (sec)		5.88		5.05	

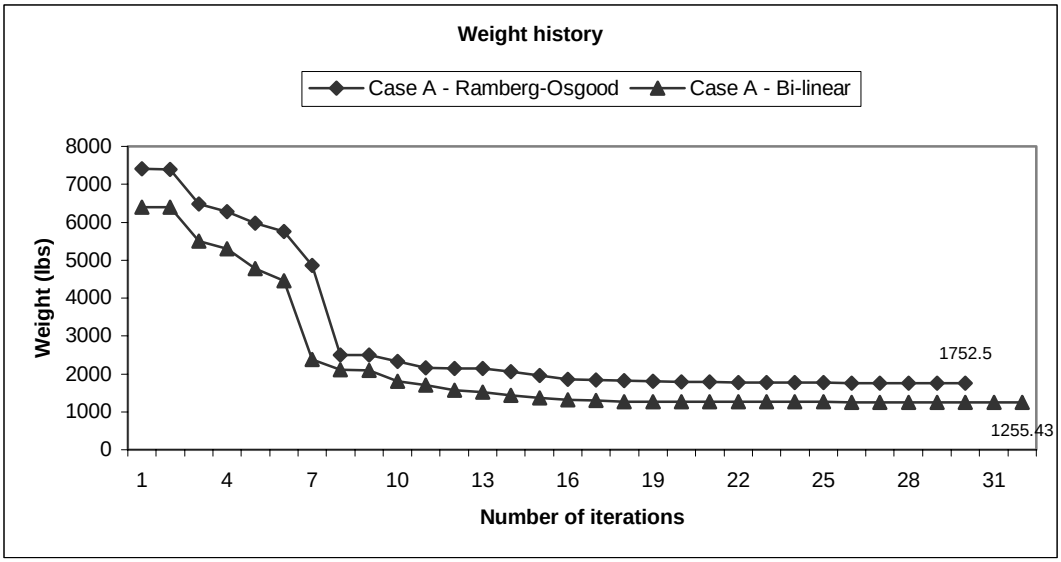

Fig. 3.8 10-bar objective history with Bi-linear and Ramberg-Osgood material

For all results in Table 3.5, the bounds of nodal X and Y displacement are enforced by not exceeding an absolute value of 10. Consequently, the optimal displacement for both Bi-linear and Ramberg-Osgood model have deflection of –10 in the Y direction at node 2. Bounds on displacements directly results higher optimum weight of Ramberg-Osgood model than linear results presented in Section 3.3.1. In other words, limitation on deflection plus hardening effect of Ramberg-Osgood curve led to higher optimum weight of Ramberg-Osgood case. Practically, those displacement bounds could be relax to give more freedom to design lighter structure in plastic region.

Two final remarks are warranted. First, DBO can easily handle any nonlinear material law while classical approach such as presented by Kaneko and Maier (1981) is only applied to Linear Strain Hardening condition. Second, computational cost of nonlinear problems as shown in section 3.3.2 and in this section are several times more than their corresponding linear problems in section 3.3.1, though they are all within an order of magnitude. The reason for different computing times between linear and nonlinear cases is that nonlinear problems are all unconstrained minimization, while linear ones are constrained problems. Using industrial optimizer DOT, constrained problems are routinely solved much more efficiently since constrained optimizers of DOT search by driving certain constraints to their boundary. The efficiency of unconstrained optimizer depends on complexity of objective descending contour of the problems solved. In conclusion, if constraint information is available in sections 3.3.2 and 3.3.3, it is expected that the computational cost of such nonlinear problems by DBO are marginally increased as compared to linear ones in section 3.3.1.

3.4 128-BAR TRUSS

This example concerns a double-layer space truss, shown in Fig. 3.9. The structural grid is 16 m by 16 m in plane size and $2\sqrt{2}$ m high. It is restrained vertically at each top node along the perimeter and in all directions at the four corner supports. The truss consists of 128 members, 41 nodes and 99 degrees of freedom. It was loaded by nodal vertical loads applied to the top nodes to simulate a uniformly distributed loading of 0.1α T/m^2, that is by nodal point loads of 1.6α T at each of the 9 interior top nodes. Adopting nodal displacement and cross-sectional areas a_i (a_i is area of the ith member) as outer and inner level design variables, respectively, we assume for both two cases considered (units are T and cm): α=15; for all elements, Young's modulus E=2000, tension yield limit=2.5 and compression 1.25; and objective function=Σa_i (since all bar lengths are equal). Further, all the a_i should be varied as $0 \le a_i \le 50$. All the deflections are limited to a maximum absolute value of 10. Two cases were investigated:

Case 1: linear elastic case

Stresses of all the members are limited within their corresponding yield limits. Therefore, 256 stress constraints are enforced in the outer level problem. (each member created two stress constraints according to upper and lower bounds)

Case 2: nonlinear material case

all the bars behave as linear hardening material in tension and elastic-perfectly-plastic in compression. Transition point of material is the member yield limit. The tension hardening modulus $H=E/8$.

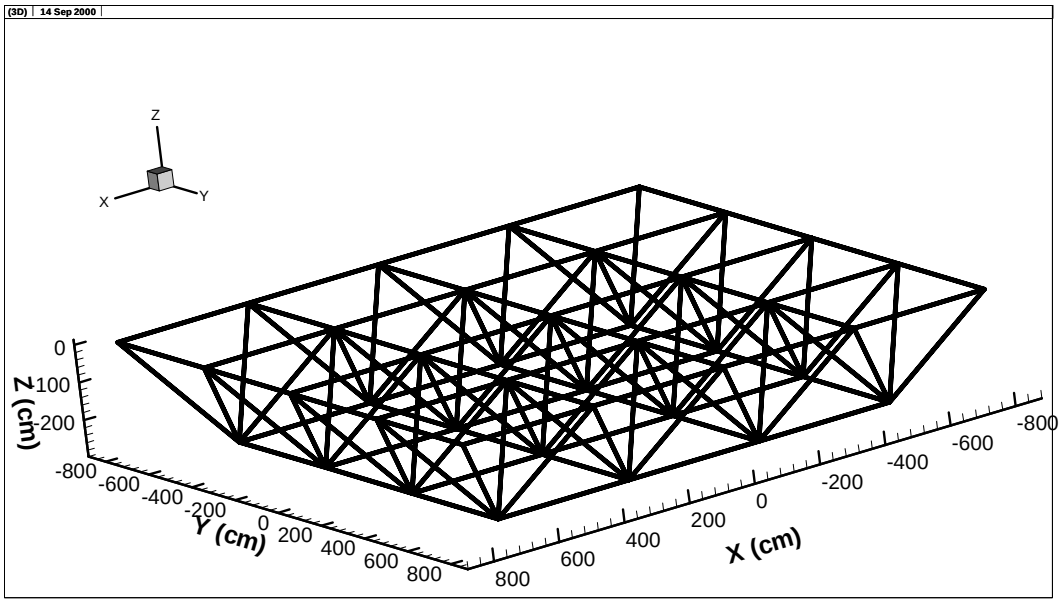

Fig. 3.9a 128-Bar double-layer space truss

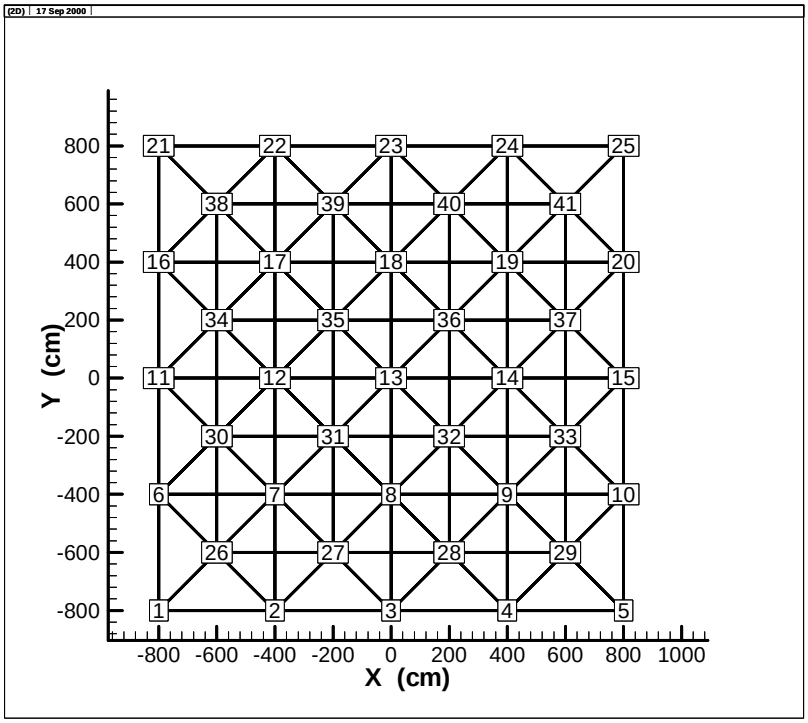

Fig. 3.9b X-Y view of 128-Bar truss

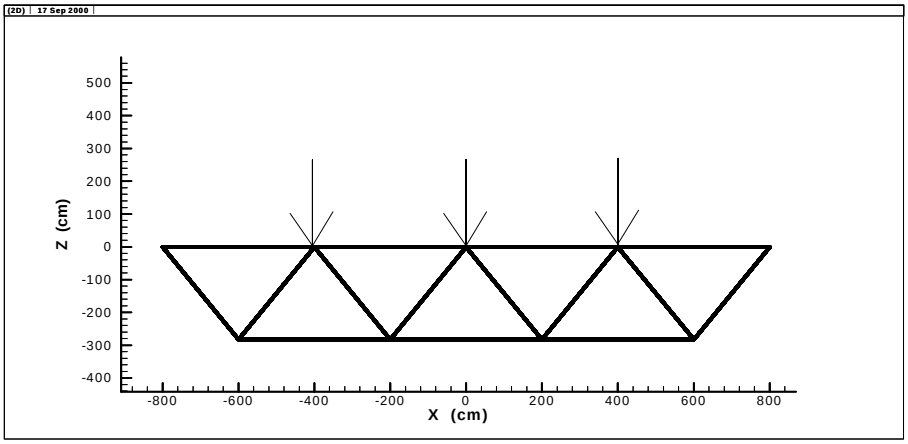

Fig. 3.9c X-Z view and loading of 128-Bar truss

For both cases, we use starting value 5 for all member areas and perform one linear structural analysis to get an initial displacement field. The outer level problems are searched in displacement design space of 99 variables. Linear case has stress constraints in the outer level problem so that Sequential Quadratic Programming solver was used. Analytical gradients of both stress constraints and objective were employed. Nonlinear case is still an unconstrained minimization problem solved by BFGS method since no constraint except bounds on displacement is considered in the outer problem. Table 3.6 lists optimum results for both cases. For simplicity, we do not report values of every member area and stress at optimum points. Fig. 3.10 plots the objective history for the nonlinear case. Fig. 3.11 and 3.12 present graphical view of optimum topological trusses for the linear and nonlinear cases, respectively. Both figures draw solid line configuration of optimum truss on background of dashed line initial truss grids.

Table 3.6 Optimum results for 128-bar truss

	Linear Case by SQP	Nonlinear Case by BFGS
Initial areas	5.0 for	all the 128 bars
Optimum areas at bound	2 bars reach 50.0	No.
Critical displacement	No.	-10 at node 13, Z direction
Maximum stress/σ_y	1.0	1.26
Degree of freedom at optimum	81	73
# of nonzero bars	84	76
Optimum weight	950.05	906.97
# of iterations	31	7
Time (sec)	166	75

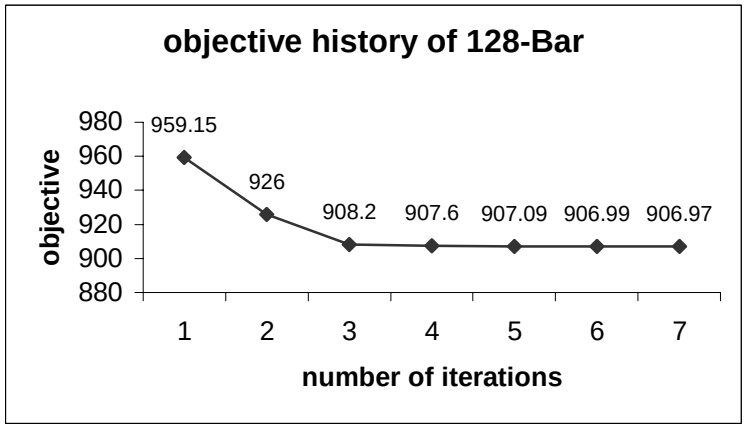

Fig. 3.10 128-bar objective history for nonlinear case

Linear case provides comparable data for studying nonlinear results. For optimum weight, linear case has 950.05, while nonlinear case had a lower one 906.97. Further investigation of the optimum results shows that 1) there are lots of critical stresses for linear case, so yield limits did restrain the stresses and thus higher optimum weight obtained, no displacement reached its bound; 2) nonlinear case has lots of stresses beyond their yield limits. Displacement at Z direction of node 13 reached its lower bound of -10 cm. It is this bound that restrained the structure to give optimum weight of 906.97. We conclude as before that lower

objective value of nonlinear case is the result of unimposing stress constraints based on yield limits.

Because of zero lower bounds on areas, for both cases the optimum structures reflect topological designs responding to external loading better than the initial design while minimizing the structural weights (see Fig. 3.11 and Fig. 3.12). However, because member can disappear from the structure if its area is zero, it is concerned whether optimum structure is a mechanism or not. First, let us look at the nonlinear case. We have 76 nonzero bars at optimum. Removal of 8 top boundary nodes 2, 4, 6, 10, 16, 20, 22, 24 (each such node has X and Y degrees of freedom (DOFs)) reduces 99 DOFs down to 83. Noticing that, if finite element analysis is performed, symmetric optimum structure and that specific loading do restrict 10 DOFs at Y direction of nodes 11-15 and X direction of nodes 3, 8, 13, 18, 23 along the X and Y symmetric lines, we could further reduce available DOFs to 83-10=73. 73 DOFs v.s. 76 bars gives a statically indeterminate structure. Thus such a loading will not lead to a mechanism at optimum. Second, linear case follows the same analysis as given above. At optimum, we have 84 nonzero bars and reduce DOFs down to 91 by removing nodes 6, 10, 16, 20. According to the same symmetric reason as to the nonlinear case, another 10 DOFs along the symmetric lines restricts down to a total of 91-10=81 DOFs. 81 DOFs v.s. 84 bars gives again a statically indeterminate structure. We also observe that the optimal topology for the linear case allows rigid body motion in X-Y plane since 4 top corner fixed nodes are useless. As far as that initial loading is applied, however, a rigid body motion will not occur. Note however that a different optimum structure will be obtained if a different external loading is applied.

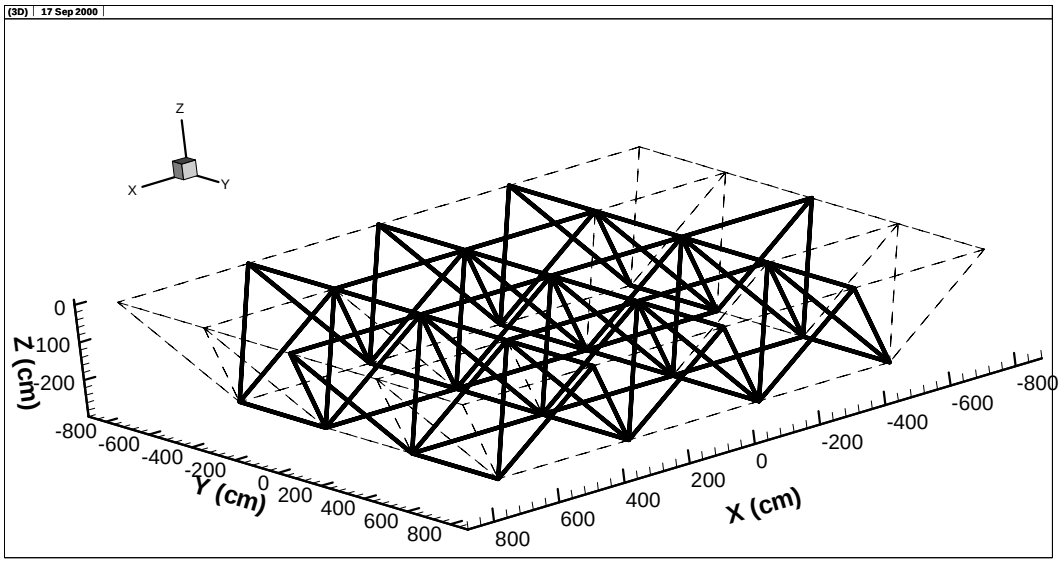

Fig. 3.11a Optimal topology of 128-Bar truss linear case

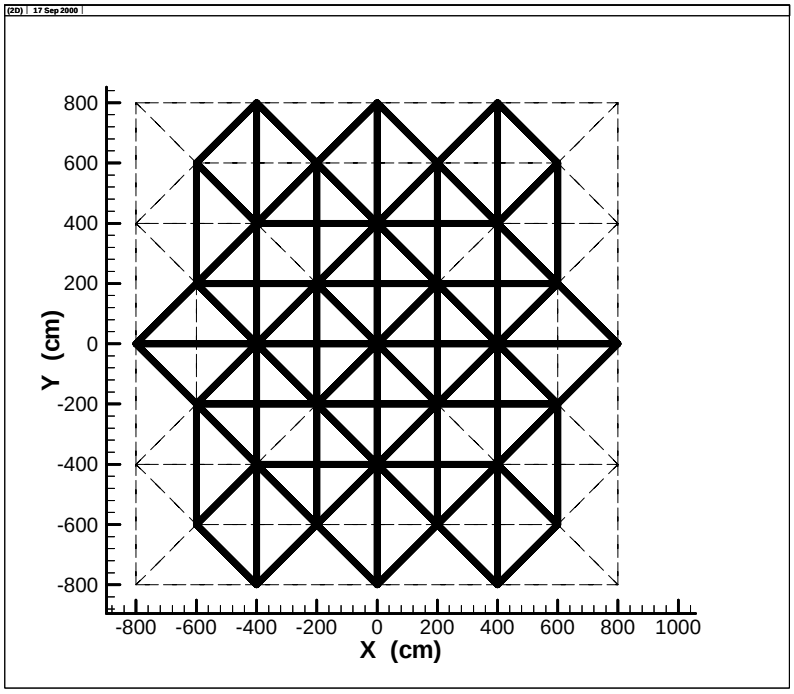

Fig. 3.11b X-Y topological view of 128-Bar truss linear case

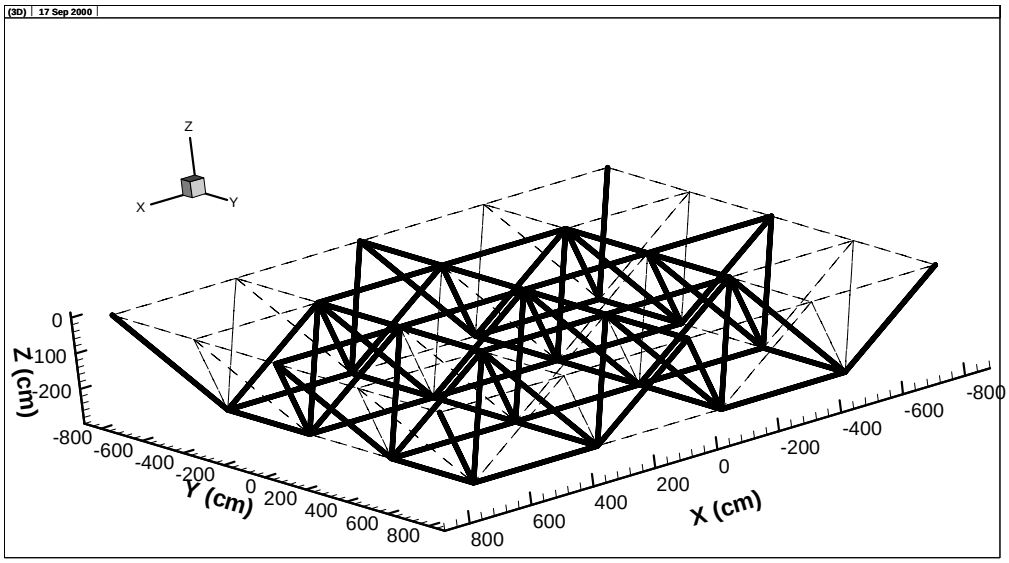

Fig. 3.12a Optimal topology of 128-Bar truss nonlinear case

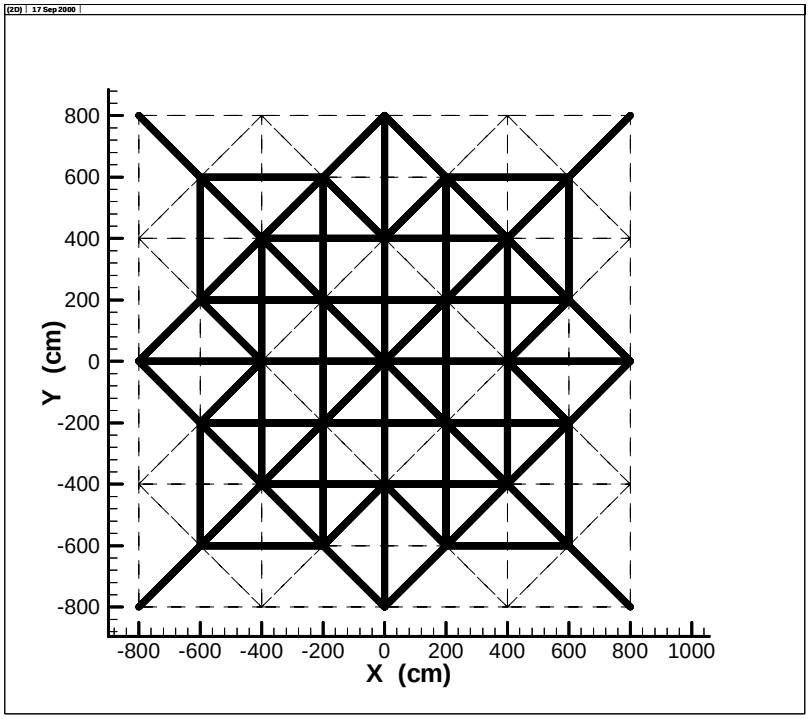

Fig. 3.12b X-Y topological view of 128-Bar truss nonlinear case